Available online at www.sciencedirect.com
ScienceDirect
Acta Biomaterialia 5 (2009) 1605–1615
Acta BIOMATERIALIA
www.elsevier.com/locate/actabiomat

Nanocomposites of bacterial cellulose/hydroxyapatite for biomedical applications

Cristian J. Grande [a,b], Fernando G. Torres [a,*], Clara M. Gomez [b], M. Carmen Bañó [c]

[a] Department of Mechanical Engineering, Catholic University of Peru, Lima 32, Peru
[b] Departament de Química Física and Institut de Ciencia dels Materials, Universitat de València, E-46100 Burjassot, Spain
[c] Departament de Bioquímica i Biologia Molecular, Facultat de Biologia, Universitat de València, E-46100 Burjassot, Spain

Received 8 May 2008; received in revised form 19 November 2008; accepted 13 January 2009
Available online 31 January 2009

Abstract

In the present work, a nanocomposite material formed by bacterial cellulose (BC) networks and calcium-deficient hydroxyapatite (HAp) powders was synthesized and characterized. The HAp nanoparticles were previously prepared by a wet chemical precipitation method, starting from aqueous solutions of calcium nitrate and di-ammonium phosphate salts. Energy-dispersive spectroscopy reveals that the prepared HAp corresponds to calcium-deficient hydroxyapatite. BC-HAp nanocomposites were prepared by introducing carboxymethylcellulose (CMC) into the bacteria culture media. HAp nanoparticles were then introduced and remained suspended in the culture medium during the formation of cellulose nanofibrils. The maximum gel thickness was obtained after 21 days of bacteria cultivation. X-ray diffractograms showed the difference of crystallinity among the materials involved in the formation of nanocomposites. The inorganic and organic bonds that corresponded to hydroxyapatite and bacterial cellulose respectively, were depicted by attenuated total reflectance Fourier transform infrared spectra. Scanning electron microscopy and atomic force microscopy measurements confirmed the formation of networks and fibres with smaller diameter corresponding to BC synthesized in the presence of CMC. Image analysis was also used to assess the orientation distributions and Feret diameters for networks of BC and BC-CMC. Thermogravimetric analysis showed that the amount of the mineral phase is 23.7% of the total weight of the nanocomposite. Moreover, HEK cells were cultivated and the biocompatibility of the materials and the cell viability was demonstrated.

Keywords: Bacterial cellulose; Hydroxyapatite; Carboxymethylcellulose; Nanocomposites

1. Introduction

Bacterial cellulose (BC) is a polysaccharide used traditionally in the food industry [1,2], later in the fabrication of reinforced paper [3] and recently it was investigated as a material for medical applications. Studies carried out in vitro and in vivo have demonstrated its biocompatibility [4,5]. Due to its good mechanical properties, water sorption capacity, porosity, stability and conformability, BC has been used in tissue engineering of cartilage [6], replacement of blood vessels in rats [7] and in the wound healing process [8,9].

BC is pure cellulose with no other components [1]. Nanocomposites based on BC can be fabricated statically either by using the synthesized BC gel or modifying the cellulose biosynthesis. For instance, BC nanocomposites for biomedical applications with improved mechanical properties were created by soaking BC on polyacrilamide and gelatin solutions [10,11]. BC-hydroxyapatite scaffolds for bone regeneration have been developed by immersing the BC gel in simulated body fluid (SBF) or in both calcium and phosphate solutions [12–16]. Furthermore, BC-polyester and BC-PVA nanocomposites were developed for potential applications as vascular implants [17,18].

* Corresponding author. Tel.: +1 5116262000; fax: +1 5116262461.
E-mail address: fgtorres@pucp.edu.pe (F.G. Torres).

1742-7061/$ - see front matter © 2009 Acta Materialia Inc. Published by Elsevier Ltd. All rights reserved.
doi:10.1016/j.actbio.2009.01.022

Some researchers have introduced different materials into the culture media of BC. BC synthesized in the presence of collagen [19] and chitosan [20] has improved properties as wound dressing and for other biomedical applications. It has been reported that BC membranes produced in the presence of carboxymethylcellulose (CMC) have better adsorption capacity of metal ions than membranes of pure BC [21–23].

However, the addition of some polymers can modify drastically the cellulose biosynthesis. The addition of CMC into the culture medium alters the crystallization and assembly of the cellulose fibrils [24]. A similar effect occurred when polyethylene oxide is added to the medium in the process for obtaining BC based nanocomposites [25].

In agitated cultures, it has been demonstrated that BC can be produced in the presence of solid particles (i.e. glass beads, paper fibres and $CaCO_3$) without affecting the rate of formation of the hydrogel [26]. Recent studies report the inclusion of silica particles of 10–20 nm and multi-walled carbon nanotubes (20–40 nm outer diameter, 10–50 μm length) into the culture medium to produce BC-nanocomposites in static cultures [27,28]. Hydroxyapatite (HAp) has been used in bone regeneration and as a substitute of bone and teeth because it is a biocompatible, bioactive, non-inflammatory, non-toxic and non-immunogenic material [29,30].

The aim of this study was to fabricate BC-HAp nanocomposites by the formation of cellulose nanofibrils in the presence of a mineral phase in a static culture. In order to suspend the HAp nanoparticles, the bacteria culture media were modified by the addition of CMC. Nanocomposites were characterized by means of X-ray diffraction (XRD), Fourier transform infrared spectroscopy (ATR-FTIR), scanning electron microscopy (SEM), atomic force microscopy (AFM), thermogravimetric analysis (TGA) and image analysis. In vitro biocompatibility and viability was assessed using HEK cells.

2. Materials and methods

2.1. Preparation of HAp powders

Hydroxyapatite (HAp) powders were prepared in vitro using a wet chemical precipitation method. $Ca(NO_3).4H_2O$ and $(NH_4)_2HPO_4$ were used as Ca and P precursors respectively, following the next basic reaction:

$$5Ca(NO_3).4H_2O + 3(NH_4)_2HPO_4 \rightarrow Ca_5(PO_4)_3OH + 6NH_4NO_3 + 19H_2O + 4HNO_3$$

Initially, 0.6 M $(NH_4)_2HPO_4$ and 1.0 M $Ca(NO_3).4H_2O$ solutions were adjusted at pH 10.2 by the addition of concentrated NH_4OH. The phosphate solution was added in drops into the stirring calcium solution at 70 °C. Stirring at this temperature was carried out for 24 h and this process was followed by further stirring for 48 h at room temperature. The resultant milky solution was filtered-washed four times with distilled water. The precipitate was dried in a vacuum oven at 60 °C for 24 h. The resultant HAp powders were milled in an agate mortar.

2.2. Preparation of BC and BC-HAp nanocomposite gels

The original culture medium for the growth of BC consisted of 1.0% (w/v) D-glucose, 1.5% (w/v) peptone, 0.8% (w/v) yeast extract and 0.3% (v/v) glacial acetic acid. The pH of the solution was adjusted to 3.5 with hydrochloric acid. In order to maintain the medium free of the action of microorganisms, it was autoclaved at 121 °C for 20 min. After the medium had cooled down, 0.01% (w/v) cycloheximide and 0.5% (w/v) absolute ethanol were added. Cycloheximide was used in order to avoid the presence of filaments while ethanol acts as an additional energy source for ATP generation enhancing thus the BC production in stationary cultures [31]. The described culture medium was used by Lisdiyanti et al. [32] and Yamada et al. [33] for the identification of acetic acid bacteria.

The strain *Gluconacetobacter saccharivorans* (LMG 1582) isolated from a Kombucha tea mat [34] was inoculated and cultivated at 30 °C for 21 days. After this period, BC gels were removed and washed with deionized water. In order to remove bacteria and eliminate the remaining culture medium, the cellulose pellicles were boiled in 1.0 M NaOH at 70 °C for 90 min followed by repetitive rinsing in deionized water.

For the formation of the new nanocomposite, HAp nanoparticles were suspended in the culture medium. In order to avoid the settling of HAp nanoparticles, the viscosity of the solution was controlled using carboxymethylcellulose sodium salt (CMC) from Acros Organics (average MW 25,0000, DS = 1.2). CMC was added to the medium in concentrations of 1.0 and 2.0% (w/v) and stirring was carried out until CMC dissolved. HAp powders were added in each vessel in concentrations of 1 and 2% (w/v) and the solutions remained under agitation overnight at room temperature. The pH was adjusted to 3.5. Both cycloheximide and ethanol were added after the sterilization process to prevent ethanol from reaching the boiling point as well as the melting of cycloheximide. Finally, an inoculum of a previously cultivated BC was introduced in the cultures. The culture conditions and washing process were the same as described above.

2.3. Samples preparation

In order to characterize the nanocomposite structures, water was removed from gels by either freeze drying, solvent exchange or hot pressing.

Pure BC, BC synthesized in the presence of 1% w/v CMC in the culture medium (BC-CMC), and nanocomposites of BC-CMC with HAp added to the culture medium in concentration of 1% w/v (BC-CMC-HAp) were frozen in liquid nitrogen (−196 °C) and freeze-dried in a Telstar

Cryodos 80 at a subliming temperature of −58 °C and a pressure of 0.18 mbar.

The solvent exchange drying method (water-ethanol-t-butyl alcohol) is suitable for preserving the original structure of BC networks [35]. BC and CMC modified BC samples were prepared using solvent exchange drying of the gels. Briefly, samples were introduced in ethanol for 45 min and then in t-butyl alcohol for 45 min. After solvent exchange, the samples were vacuum dried.

Gels of pure BC, BC-CMC (1% w/v) and nanocomposites of BC-CMC-HAp were dehydrated by hot pressing (0.015 MPa) at 105 °C during 5 min in order to obtain sheets for analysing their crystallinity and cell viability.

2.4. Characterization

A few milligrams of the freeze-dried samples and pure HAp powders were evaluated separately with a FTIR-ATR, Nicolet Nexus 470 equipped with a diamond probe. 64 scans were used in the reflectance mode at a resolution of 8 cm^{-1} in the range from 4000 to 400 cm^{-1}. The data were analysed with Omnic software.

In order to analyse the microstructure of the freeze-dried samples, scanning electron microscopy (SEM) was used. BC-based samples and HAp powders were previously sputter coated with Au-Pd. Energy-dispersive spectroscopy (EDS) was used to determine the relation Ca/P of the HAp powders. RÖNTEC-Shell and RÖNTEC-Tool systems were used to acquire and process the microanalysis, respectively. SEM and EDS were carried out using a field emission SEM Hitachi S4100 at 15 and 20 kV, respectively.

Image analysis of the SEM micrographs was performed by using the ImageJ software (Research Services Branch, National Institute of Mental Health, National Institutes of Health, NHI, USA). The diameter of the fibrils, their orientation and the pore size of the BC surface in contact with the culture medium [36] were assessed. In order to determine the orientation of the fibrils, the fibrils were replaced by segments connecting the junction points and the angles between the segments and the x axis were recorded. The Feret diameter (i.e. the maximum distance between two parallel tangents) was taken as the measure of the pore size.

Freeze-dried samples were analysed by thermogravimetric analysis (TGA) in order to determine the composition of HAp in the BC-HAp nanocomposites and the rate of change in weight of BC based materials and HAp powders. Also, washed gels were analysed by TGA in order to determine the amount of water. A Setaram Setsys 92-12 was used in the range 50–900 °C with a heating rate of 10 °C min^{-1}.

Measurements of the surfaces of BC and BC-CMC samples in contact with the culture medium and obtained by the solvent exchange drying method were carried out using AFM (easyScan 2, Nanosurf AG, Switzerland) in the dynamic mode. A cantilever with a nominal spring constant of 42 N m^{-1}, resonance frequency of 179 kHz and a tip radius lower than 10 nm was used.

For X-ray diffraction (XRD) and cell seeding studies, hot pressed BC, BC-CMC and BC-CMC-HAp samples were prepared. Using a Seifert XRD 3003 TT diffractometer, Ni-filtered CuKα radiation ($\lambda = 0.1542$ nm) was produced at 40 kV and 40 mA. Scattered radiation was detected in the angular range of 2.5–70° (2θ) in steps of 0.08° (2θ). The data were analysed using Analyse and DRX-Win softwares.

2.5. Cell culture

HEK cells were used to assess the biocompatibility and viability of the materials of the nanocomposites. Previous to cell seeding, samples were UV sterilized overnight. The cells were cultured in Dulbecco's Modified Eagle's Medium (DMEM, Gibco) supplemented with 10% fetal bovine serum (FBS, Gibco), 1% penicillin-streptomicyn (P/S) and 0.1% fungizone in a humidified atmosphere at 37 °C and 5% CO_2. Medium was removed and cells were washed with phosphate buffered saline (PBS, Gibco). Cells were trypsnized in 0.2% trypsin solution and 5 ml of culture medium was added. The cell suspension was centrifuged at 1500 rpm for 3 min and the medium was removed. Cells were re-suspended with 6 ml of culture media. 1 ml of cell suspension was seeded directly onto the materials inside the tissue culture plate (TCP). Furthermore, 3 ml of fresh culture medium was added covering all parts of the material. A TCP was used as a control.

After 1 day of culture, images were taken for analysing biocompatibility. Furthermore, materials were removed from TCP and put into new ones with fresh culture medium for analysing if cells are stacked on the surfaces. For the viability analysis, cells of the original TCP were trypsinized with 300 μl trypsin solution. Also, 700 μl of fresh culture medium were used to stop the reaction. 100 μl was put into eppendorf tubes with the same volume of trypan blue. These solutions were put into a Neubauer camera and analysed by optical microscopy.

3. Results and discussion

Morphological characterization was used in order to further understand the effect of the HAp phase on the formation of the BC network. Fig. 1a shows the morphology of the HAp powders obtained by the described wet chemical process. Powders appeared free of other substances and agglomerated in micrometric particles. Also, micrometric particles are composed of particles at the nano level [37].

Fig. 1b shows a typical bacterial cellulose network of the surface exposed to the culture medium. In the presence of CMC at 1% w/v in the culture media, bacteria form cellulose fibrils with smaller diameters than those occurring in pure BC (Fig. 2). The average diameter of BC fibres was determined in 117.76 nm ± 29.58 nm; and the average diameter of BC fibres produced in the presence of CMC (1% w/v) was 60.90 nm ± 12.63 nm.

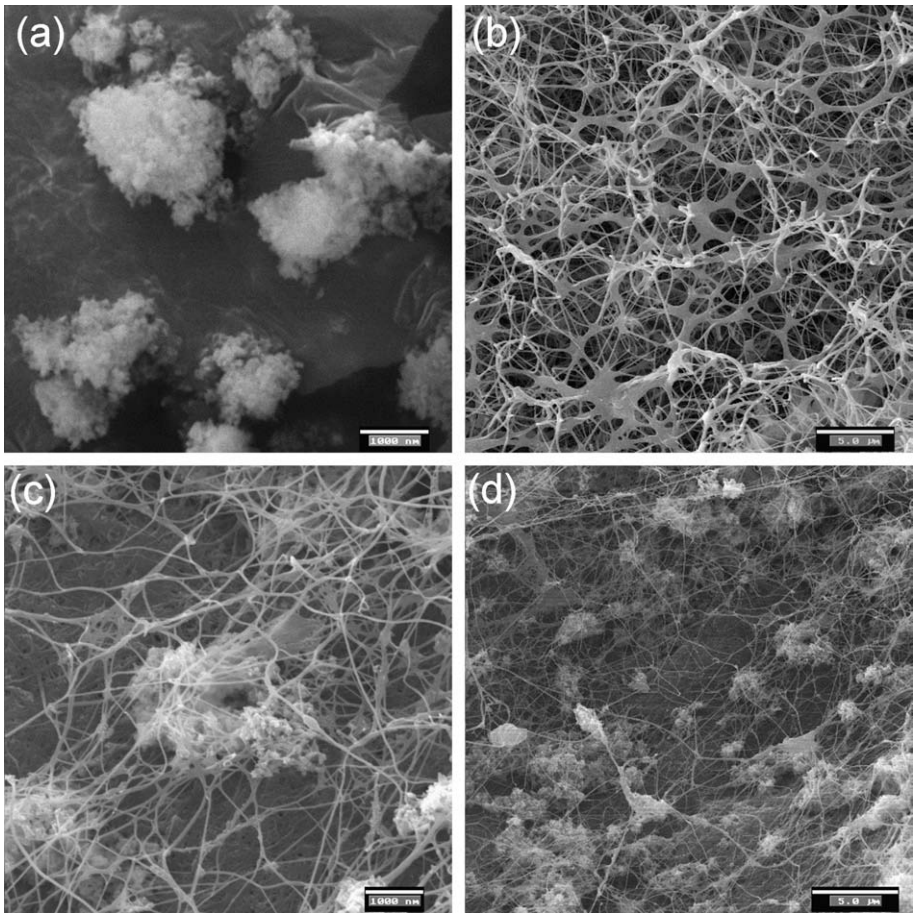

Fig. 1. SEM micrographs of: (a) surface of precipitated HAp powders; (b) original cellulose network; (c) HAp powders inside the cellulose network; (d) distribution of HAp powders in cellulose network.

The water extraction method influences the morphology of BC networks. A previous study carried out in our laboratory indicates that the fibre diameter of pure BC compressed sheets is in the range 100–200 nm [34]. The solvent exchange drying method (water-ethanol-t-butyl alcohol) was carried out in order to maintain the cellulose fibre structure [35]. AFM measurements of these samples (Fig. 3) confirmed SEM measurements. The average diameter of BC and BC-CMC (1% w/v) were 119.90 nm ± 49.97 nm and 70.44 ± 30.04, respectively. Thus, unmodified BC fibres are larger than BC-CMC fibres.

It should be noted that these results differ from other reported in the literature where BC-CMC fibres are larger than the unmodified BC ones due to the aggregation of bundles produced by the presence of a compatible polymer [38,39]. The differences reported here could be attributed to the effect of CMC on the strain of bacteria used in our experiments; however, further work would be needed to confirm this.

Other BC network properties assessed were the pore size and the orientation of the fibres (angle between the x-axis and the fibre). The distribution of the angles found is depicted in Fig. 4a. The average value of the angle is similar for both BC and BC-CMC network and is equal to 84.30° and 84.73°, respectively. In contrast, the pore size distribution (Fig. 4b) and the average pore size are different. The average pore size in BC and BC-CMC (1% w/v) networks are 0.5230 μm ± 0.2733 μm and 0.7733 μm ± 0.5238 μm, respectively. These results are in agreement with data for the water holding capacity of BC and BC-CMC reported previously by other authors [22,23,40].

The Ca/P ratio for the stoichiometric HAp is 1.67. Calcium-deficient HAp is of greater biological interest because this is the type of HAp almost always present in physiological media [41]. An EDS (energy-dispersive spectroscopy) spectrum of the HAp produced is shown in Fig. 5. The Ca/P ratio determined by the RONTEC software was 1.60, indicating that the mineral phase is calcium-deficient HAp.

The diameter of the HAp particles present in the nanocomposites was compared with the diameter of the synthesized HAp particles added to the culture medium (Fig. 6). The average diameter of the particles in the nanocomposites (2.59 μm ± 1.25 μm) was lower than the average diameter of the HAp particles added to the medium (3.34 μm ± 2.25 μm). This difference should be due to the fact that the larger HAp particles in the culture medium sank to the bottom of the vessel in accordance with the Stoke's settling theory.

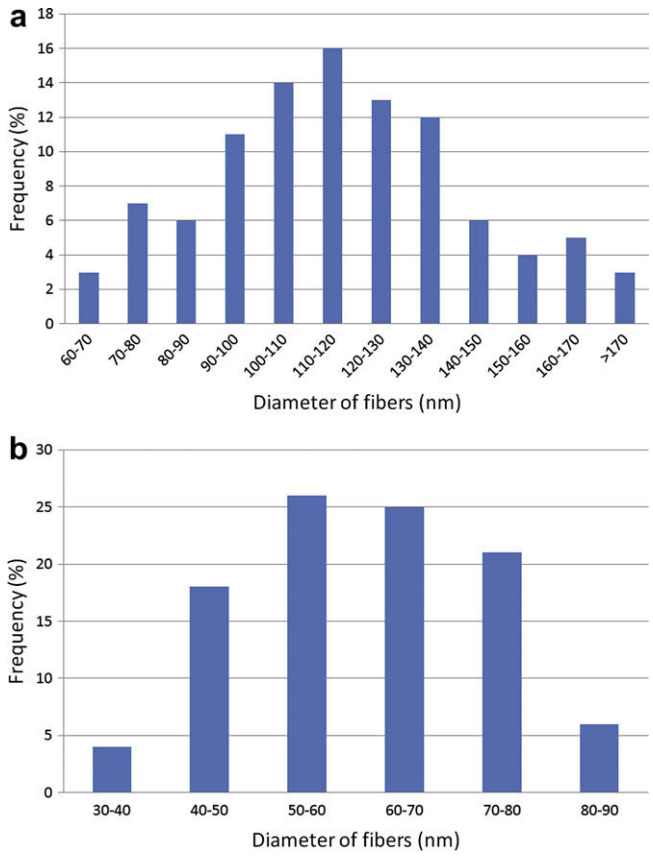

Fig. 2. Distribution of diameter of fibrils corresponding to pure (a) BC and (b) BC–CMC (1% w/v).

CMC increases the viscosity of the culture medium [42] and improves the capability of the solution to retain the HAp particles in suspension. Without CMC, the HAp particles would fall to the bottom of the vessel where the BC gel is produced. The Stokes settling theory has been used to estimate the settling velocity of the HAp particles in the culture medium. The settling velocity is directly proportional to the particle size and reduces with the viscosity of the medium. Thus, the settling velocity of HAp in the culture medium containing CMC (v_2) can be related to the settling velocity of HAp in the culture medium without CMC (v_1) by the Eq. (1):

$$\frac{v_1}{v_2} = \frac{\mu_2}{\mu_1}, \tag{1}$$

where μ_2 is the dynamic viscosity of the culture medium containing CMC and μ_1 is the dynamic viscosity of the culture medium without CMC. According to the technical specifications of the CMC provided, μ_2/μ_1 is around 1500–3000 in a 2% solution at 25 °C. Thus, the settling velocity of HAp in the culture medium containing CMC is around 3.5×10^{-9} m s^{-1} (i.e. HAp particles would fall 0.3 mm day^{-1}). Thus, HAp powders can be trapped in the cellulose network (Fig. 1c and d).

The addition of CMC at concentrations of 2% (w/v) produces BC-HAp nanocomposites of very thin thickness (0.5 mm). These gels were not integral structures and could not be removed without suffering damage. This structure is similar to other ones based on CMC reported by Brown [40]. On the other hand, studies indicate that strains in the presence of different amounts of CMC with different degree of substitution have increased yields, due probably to the presence of the additional carbon sources in CMC. In this study, gels of about 8 mm and 99.15% of water content were obtained. Since the volume of the gels is about a fourth of the volume of the vessel containing the culture medium and assuming that CMC was uniformly solubilized in the culture medium, it was estimated that about 0.25% of the initial CMC was incorporated into the final nanocomposites.

The ATR-FTIR spectra of the HAp powders, CMC-HAp, BC, BC-CMC, and nanocomposites of BC-CMC-HAp are depicted in Fig. 7. A usual characteristic of the modification of cellulose networks by the addition of CMC is the decreasing intensity of the band corresponding to the cellulose type Iα (750 cm^{-1}) [43].

In the analysed CMC-HAp freeze-dried suspension, the typical band of CMC corresponding to (ν COONa) appears at 1599 cm^{-1}. In this spectrum there is a predominance of the chemical groups corresponding to HAp at 1032, 602 and 563 cm^{-1}. The interaction between CMC and HAp is confirmed by the fact that the peak at

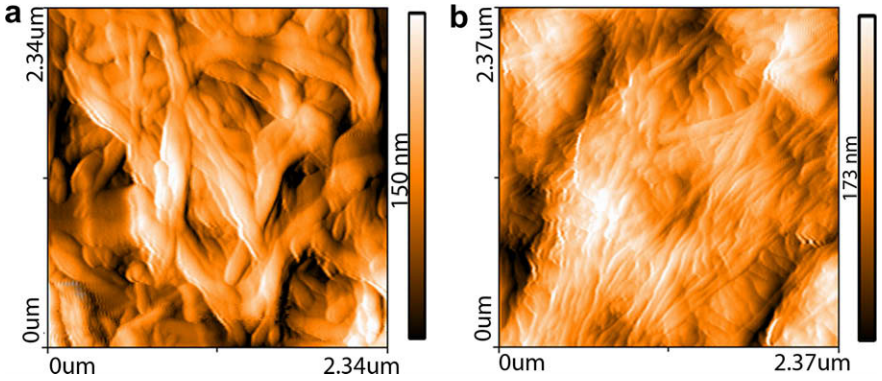

Fig. 3. AFM images of: (a) BC; (b) BC produced in the presence of 1% w/v CMC.

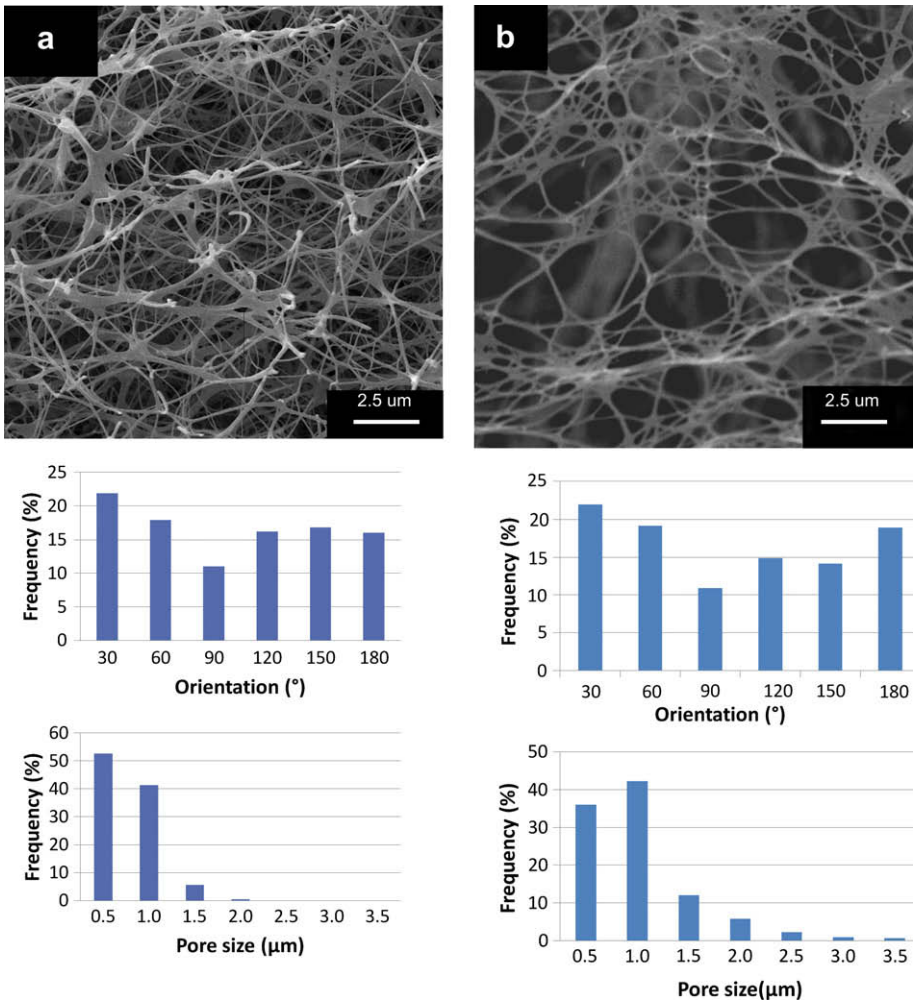

Fig. 4. Orientation and diameter distribution of (a) pure BC and (b) BC produced in the presence of 1% w/v CMC.

1024 cm^{-1} in the spectrum of pure HAp shifted to 1032 cm^{-1} in the spectrum of CMC-HAp. Furthermore, in the BC-CMC-HAp nanocomposites the bands at 1032 and 963 cm^{-1} that correspond to asymmetric and symmetric modes of the P–O bonds for the phosphate groups were present. Intensities at 602 and 563 cm^{-1} were attributed to the bending mode of the O–P–O bonds of the phosphate groups [44,45]. In the nanocomposites there are reduced intensities at 1160 and 1050 cm^{-1} that correspond to C–O–C asymmetric stretching and C–O bond stretching modes of BC, respectively [46,47]. Thus, the presence of well bonded chemical groups of BC and HAp improves the stabilization of the nanocomposites.

As with CMC-HAp, in the nanocomposites IR spectra a predominance of the HAp spectra with regard to BC and BC-CMC can be observed. Furthermore, typical HAp peaks detected in the nanocomposites have lower intensities than those corresponding to pure HAp. This could be due to a reduction of crystallinity with respect to pure HAp. This information is confirmed by XRD, since the crystallinity of the mineral phase in the final nanocomposites is reduced with respect to pure HAp (Fig. 8).

XRD peaks observed at 25.8°, 31.8°, 32.9°, 34.0° 39.7°, 46.6°, 49.4° and 53.1° correspond to pure HAp (Fig. 8) [48]. On the other hand, BC present intensities at 14.5° and 22.6°. The broad diffraction peaks indicate that BC is not totally a crystalline material [49]. Furthermore, BC modified with CMC at 1% w/v present diffraction planes at the same values of pure BC. However, there is a reduction in the values of the crystallite size of BC because the half width of each peak is broadened. Yamamoto et al. [43] claimed that a decrease in crystallite size is in good agreement with the decrease in average microfibril size determined by TEM. This is in accordance with our results in which the average diameter of BC-CMC fibrils is almost 50% smaller than the same value corresponding to pure BC.

The nanocomposites of BC-CMC-HAp have the two typical peaks of BC-CMC. Also, the broad intensities attributed to the crystals of the HAp powders in the nanocomposites indicate low values of crystallinity of HAp present in BC. These XRD data are in accordance to those of BC-HAp nanocomposites obtained by the immersion of BC pellicles in SBF and calcium-phosphate solutions [12–14,16].

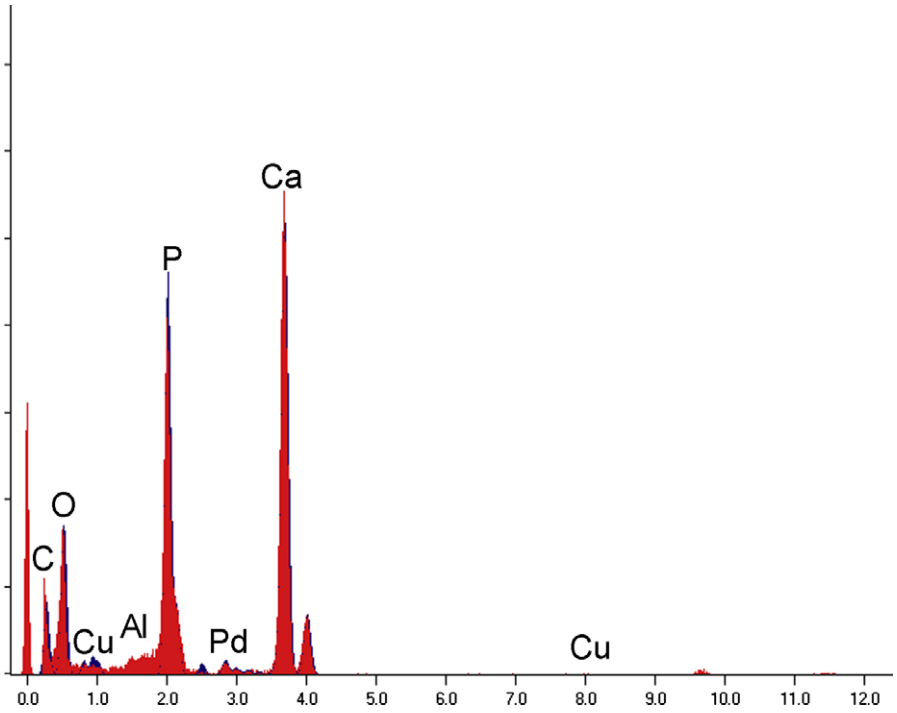

Fig. 5. EDS spectrum of prepared hydroxyapatite.

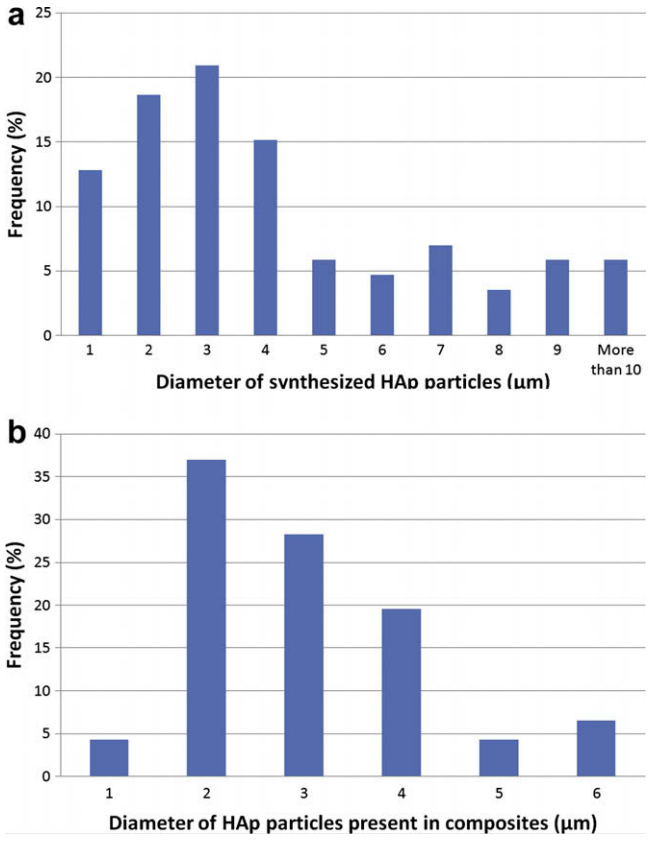

Fig. 6. Distribution of diameter for (a) synthesized HAp powders and (b) HAp present in the nanocomposites.

The TG thermograms for the prepared materials are shown in Fig. 9. The first thermogram (Fig. 9) indicates that up to 900 °C, HAp loss 7.2% of its initial weight. Also, in this thermogram there was no phase transformation, indicating the stability of this mineral at high temperatures. Fig. 9 shows that the total weight loss of the BC-HAp nanocomposites was 76.3% due to dehydroxylation and decomposition of organic macromolecules. Furthermore, it can be seen that after 675 °C there was no more weight loss. This indicates that all the organic components were decomposed under this temperature. In this manner, the material remains stable up to 900 °C due to the presence only of HAp. Thus, the mineral phase in the nanocomposites constitutes 23.7% of the total weight.

Fig. 10 shows optical microscopy images for cultures of one day of HEK cells in the presence of thin sheets of BC (Fig. 10a), BC synthesized with 1% w/v CMC (Fig. 10b), nanocomposite of BC-HAp (Fig. 10c) and control (Fig. 10d). Cells proliferated in all cases. Confluence was achieved after two days of culture.

Fig. 11 shows the same materials removed from their original culture media and placed into a new TCP in the presence of fresh culture media. From these pictures it can be inferred that the most part of living cells were not in the thin sheets but in the TCP surfaces. On the other hand, the viability analysis shows 86.8%, 95.1% and 97.2% for media in which were present BC, BC produced with 1% w/v CMC and BC-HAp nanocomposites, respectively. The pore size, pore orientation, fibre structure and fibre diameter of scaffolds have an influence on cell behaviour and development of artificial skin and other type of tissues [50]. The increased cell viability of HEK cells in BC-CMC with respect to BC can be attributed

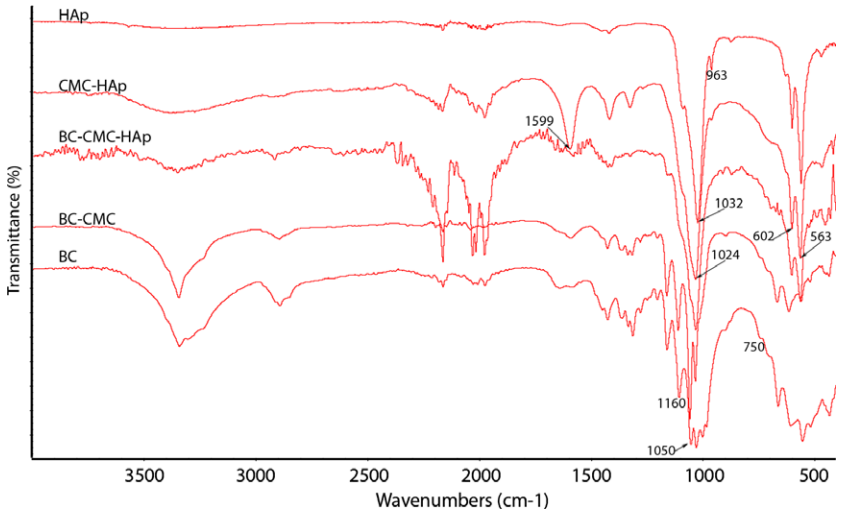

Fig. 7. ATR-FTIR spectra of HAp, CMC at 1% w/v–HAp at 1% w/v, BC-HAp nanocomposites, BC modified with 1% w/v CMC and BC.

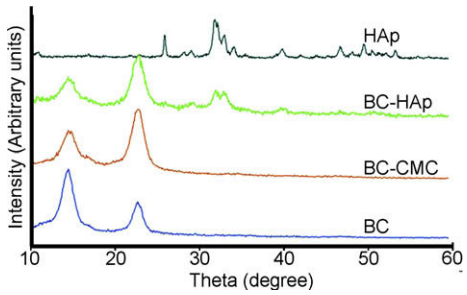

Fig. 8. X-ray diffractograms of wet chemical synthesized HAp; BC-HAp nanocomposites; BC modified with 1% w/v CMC and BC.

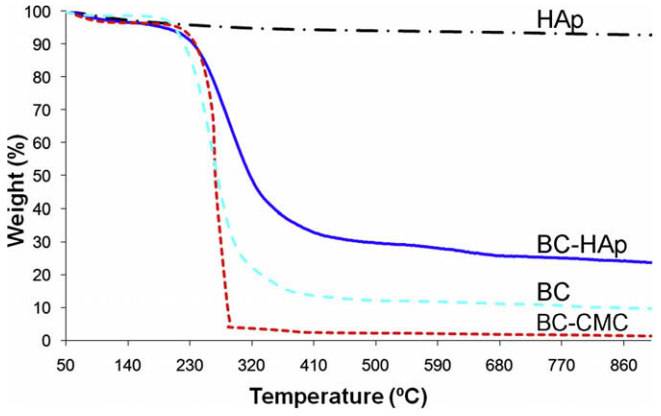

Fig. 9. TG thermograms for HAp; BC-HAp nanocomposite; BC and BC modified with 1% w/v CMC.

to the smaller diameters and increased pore sizes obtained in BC produced in the presence of CMC. Also, HAp has the ability to form a direct chemical bond with surrounding tissues [29]. The increased cell viability in BC-HAp composites is attributed to this property. Though living cells were not present on the surface of synthesized materials, these can be considered as biocompatible due to the presence of cells in the same culture media. Further studies in surface modification [4] for improving the adhesion of living cells to these materials are necessary for characterizing these materials as potential scaffolds for tissue engineering.

4. Conclusions

Nanocomposites of BC-HAp were produced by introducing the mineral phase into the bacteria culture medium during the formation of cellulose fibrils. For this purpose, CMC (1% w/v) was used in order to suspend the HAp nanoparticles by controlling the viscosity of the culture medium. By using CMC, the average diameter of cellulose fibres is almost 50% lower than the average diameter of the unmodified BC fibres. This result was attributed to the effect that some polysaccharides cause in the fibre assembly during the cellulose biosynthesis. The fibre orientation distributions of BC and BC-CMC images demonstrated that freeze-dried BC consists of randomly assembled nanofibres forming a network. Also, the pore size of BC increases 47.8% when CMC is added to the culture media. Image analysis of the HAp particles before and after the synthesis of the nanocomposites suggest that an amount of HAp powders (22%) did not get included in the final nanocomposites.

FTIR analysis demonstrates the interactions between functional groups of HAp and BC in the final nanocomposites. In addition, XRD tests proved that the nanocomposites have reduced crystallinity compared to pure HAp. Thus, chemical bonds between the components improve the chemical stabilization of this nanocomposite for biomedical applications. Furthermore, TGA analysis demonstrated that the inorganic phase represents 23.7% of the total weight of the nanocomposite.

The biocompatibility and cell viability of the nanocomposites prepared was confirmed by HEK cell seeding. The pore size and fibre diameter of BC networks are

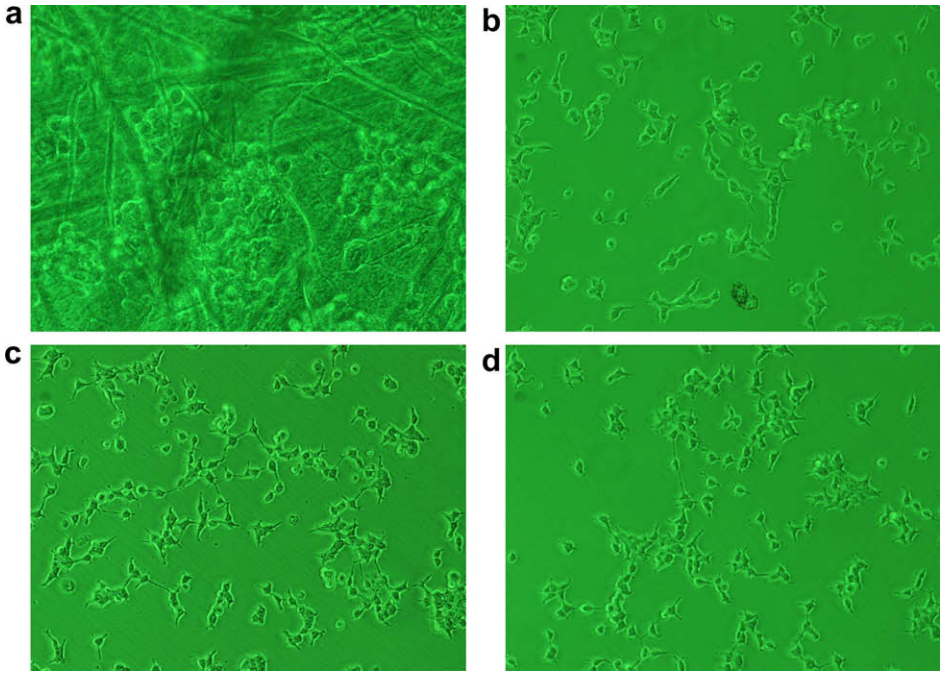

Fig. 10. Optical micrographs of HEK cells for one day of culture in (a) BC; (b) BC modified with CMC (1% w/v); (c) nanocomposite of BC-Hap; and (d) control plate.

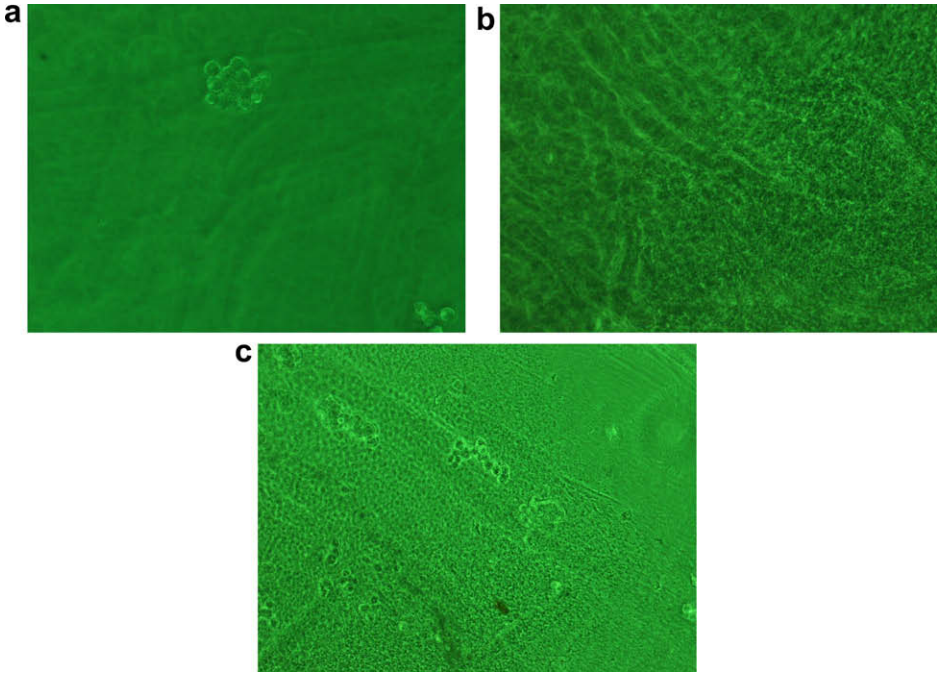

Fig. 11. Optical micrographs of sheets of (a) BC; (b) BC modified with CMC (1% w/v) and (c) nanocomposite of BC-HAp removed from culture media with some cells stacked to their surfaces.

influenced by the water extraction method. Studies reported by Bhattarai et al. [50] and Yang et al. [51] indicate that the pore size and fibre diameter of scaffolds influence the cell growth; however further studies are needed in order to analyse the influence of the network geometry in cellular response of the BC scaffolds dehydrated by freeze drying and solvent exchange.

Different type of micro/nano particles can be suspended by varying the viscosity of the culture media. Thus, different types of solid particles can be added to the medium for the formation of nanocomposites with BC. Furthermore, the biocompatibility of the materials and the bioactivity of HAp are factors that make this nanocomposite a material with potential biomedical applications.

Acknowledgements

CJG would like to thank the International Relations Office (Oficina de Relaciones Internacionales) of the University of Valencia for the financial support received. The authors would also like to thank the Direction of Academic Research of the Catholic University of Peru (DAI), The International Foundation for Science (IFS, Sweden) and Generalitat Valenciana, Conselleria de Empresa, Universidad y Ciencia, project number ARVIV/2007/101. O. Troncoso is acknowledged for experimental assistance with Image Analysis software.

References

[1] Iguchi M, Yamanaka S, Budhiono A. Bacterial cellulose – a masterpiece of nature's arts. J Mater Sci 2000;35:261–70.
[2] Okiyama A, Motoki M, Yamanaka S. Bacterial cellulose II: processing of the gelatinous cellulose for food materials. Food Hydrocolloids 1992;6:479–87.
[3] Yamanaka S, Watanabe K, Kitamura N, Iguchi M, Mitsuhashi S, Nishi Y, et al. The structure and mechanical properties of sheets prepared from bacterial cellulose. J Mater Sci 1989;24:3141–5.
[4] Watanabe K, Eto Y, Takano S, Nakamori S, Shibai H, Yamanaka S. A new bacterial cellulose substrate for mammalian cell culture. Cytotechnology 1993;13:107–14.
[5] Helenius G, Backdahl H, Bodin A, Nannmark U, Gatenholm P, Risberg B. In vivo biocompatibility of bacterial cellulose. J Biomed Mater Res A 2006;76:431–8.
[6] Svensson A, Nicklasson E, Harrah T, Panilaitis B, Kaplan DL, Brittberg M, et al. Bacterial cellulose as a potential scaffold for tissue engineering of cartilage. Biomaterials 2005;26:419–31.
[7] Klemm D, Schumann D, Udhardt U, Marsch S. Bacterial synthesized cellulose – aritificial blood vessels for microsurgery. Prog Polym Sci 2001;26:1561–603.
[8] Czaja W, Krystynowicz A, Bielecki S, Brown RM. Microbial cellulose – the natural power to heal wounds. Biomaterials 2006;27:145–51.
[9] Czaja W, Young DJ, Kawecki M, Brown RM. The future prospects of microbial cellulose in biomedical applications. Biomacromolecules 2007;8:1–12.
[10] Yasuda K, Ping Gong J, Katsuyama Y, Nakayama A, Tanabe Y, Kondo E, et al. Biomechanical properties of high-toughness double network hydrogels. Biomaterials 2005;26:4468–75.
[11] Nakayama A, Kakugo A, Ping Gong J, Osada Y, Takai M, Erata T, et al. High mechanical strength double-network hydrogel with bacterial cellulose. Adv Funct Mater 2004;14:1124–8.
[12] Hong L, Wang YL, Jia SR, Huang Y, Gao C, Wan YZ. Hydroxyapatite/bacterial cellulose nanocomposites synthesized via a biomimetic route. Mater Lett 2006;60:1710–3.
[13] Wan YZ, Hong L, Jia SR, Huang Y, Zhu Y, Wang YL, et al. Synthesis and characterization of hydroxyapatite-bacterial cellulose nanocomposites. Compos Sci Technol 2006;66:1825–32.
[14] Wan YZ, Huang Y, Yuan CD, Raman S, Zhu Y, Jiang HJ, et al. Biomimetic synthesis of hydroxyapatite/bacterial cellulose nanocomposites for biomedical applications. Mater Sci Eng C 2007;27:855–64.
[15] Bodin A, Gustafsson L, Gatenholm P. Surface engineered bacterial cellulose as template for crystallization of calcium phosphate. J Biomater Sci Polym Ed 2006;17:435–47.
[16] Hutchens SA, Benson RS, Evans BR, O'Neill HM, Rawn CJ. Biomimetic synthesis of calcium-deficient hydroxyapatite in a natural hydrogel. Biomaterials 2006;27:4661–70.
[17] Charpentier PA, Maguire A, Wan WK. Surface modification of polyester to produce a bacterial cellulose-based vascular prosthetic device. Appl Surf Sci 2006;252:6360–7.
[18] Millon LE, Mohammadi H, Wan WK. Anisotropic polyvinyl alcohol hydrogel for cardiovascular applications. J Biomed Mater Res B 2006;79:305–11.
[19] Wiegand C, Elsner P, Hipler UC, Klemm D. Protease and ROS activities influenced by a nanocomposite of bacterial cellulose and collagen type I in vitro. Cellulose 2006;13:689–96.
[20] Ciechanska D. Multifunctional bacterial cellulose/chitosan nanocomposite materials for medical applications. Fibres Text East Eur 2004;12:69–72.
[21] Chen S, Zou Y, Yan Z, Shen W, Shi S, Zhang X, et al. Carboymethylated-bacterial cellulose for copper and lead ion removal. J Hazard Mater 2008. 10.1016/j.jhazmat.2008.04.098.
[22] Seifert M, Hesse S, Kabrelian V, Klemm D. Controlling the water content of never dried and reswollen bacterial cellulose by the addition of water-soluble polymers to the culture medium. J Polym Sci A Polym Chem 2004;42:463–70.
[23] Sakairi N, Suzuki S, Ueno K, Han SM, Nishi N, Tokura S. Biosynthesis of hetero-polysaccharides by *Acetobacter xylinum* – synthesis and characterization of metal-ion adsorptive properties of partially carboxymethylated cellulose. Carbohydr Polym 1998;37:409–14.
[24] Haigler CH, White AR, Brown RM, Cooper KM. Alteration of in vivo cellulose ribbon assembly by carboxymethylcellulose and other cellulose derivatives. J Cell Biol 1982;94:64–9.
[25] Brown EE, Laborie MPG. Bioengineering bacterial cellulose/poly(ethylene oxide) nanocomposites. Biomacromolecules 2007;8:3074–81.
[26] Serafica G, Mormino G, Bungay H. Inclusion of solid particles in bacterial cellulose. Appl Microbiol Biotechnol 2002;58:756–60.
[27] Yano S, Maeda H, Nakajima M, Hagiwara T, Sawaguchi T. Preparation and mechanical properties of bacterial cellulose nanocomposites loaded with silica nanoparticles. Cellulose 2008;15:111–20.
[28] Yan Z, Chen S, Wang H, Wang B, Wang C, Jiang J. Cellulose synthesized by *Acetobacter xylinum* in the presence of multi-walled carbon nanotubes. Carbohydr Res 2008;343:73–80.
[29] Murugan R, Ramakrishna S. In situ formation of recombinant humanlike collagen-hydroxyapatite nanohybrid through bionic approach. Appl Phys Lett 2006;88:193124.
[30] Thomas V, Dean DR, Jose MV, Mathew B, Chowdhury S, Vohra YK. Nanostructured biocomposite scaffolds based on collagen coelectrospun with nanohydroxyapatite. Biomacromolecules 2007;8:631–7.
[31] Krystynowicz A, Czaja W, Wiktorowska-Jezierska A, Goncalves-Miskiewicz M, Turkiewicz M, Bielecki S. Factors affecting the yield and properties of bacterial cellulose. J Ind Microbiol Biotechnol 2002;29:189–95.
[32] Lisdiyanti P, Kawasaki H, Widyastuti Y, Saono S, Seki T, Yamada Y, et al. Kozakia baliensis gen. nov., sp. Nov., a novel acetic acid bacterium in the α-proteobacteria. Int J Syst Evol Microbiol 2002;52:813–8.
[33] Yamada Y, Hosono R, Lisdiyanti P, Widyastuti Y, Saono S, Uchimura T, et al. Identification of acetic acid bacteria isolated from Indonesian sources especially of isolates classified in the genera Gluconobacter. J Gen Appl Microbiol 1999;45:23–8.
[34] Grande CJ, Torres FG, Gomez CM, Troncoso OP, Canet-Ferrer J, Martínez-Pastor J. Morphological characterization of bacterial cellulose-starch nanocomposites. Polym Polym Compos 2008;16:181–5.
[35] Kuga S, Kim DY, Nishiyama Y, Brown RM. Nanofibrillar carbon from native cellulose. Mol Cryst Liq Cryst 2002;387:13–9.
[36] Nge TT, Sugiyama J. Surface functional group dependent apatite formation on bacterial cellulose microfibrils network in a simulated body fluid. J Biomed Mater Res A 2007;81:124–34.
[37] Pretto M, Costa AL, Landi E, Tampieri A, Galassi C. Dispersing behavior of hydroxyapatite powders produced by wet chemical synthesis. J Am Ceram Soc 2003;86:1534–9.
[38] Klemm D, Schumann D, Kramer F, Hebler N, Hornung M, Schmauder H-P, et al. Nanocelluloses as innovative polymers in research and application. Adv Polym Sci 2006;205:49–96.

[39] Hirai A, Tsuji M, Yamamoto H, Horii F. In situ crystallization of bacterial cellulose III. Influences of different polymeric additives on the formation of microfibrils as revealed by transmission electron microscopy. Cellulose 1998;5:201–13.
[40] Brown RM. Microbial cellulose modified during synthesis. US Patent 4942128; 1990.
[41] Vallet-Regi M, Rodriguez-Lorenzo LM, Salinas AJ. Synthesis and characterization of calcium-deficient hydroxyapatite. Solid State Ionics 1997;101–103:1279–85.
[42] Majewicz TG, Erazo-Majewicz PE, Podlas TJ. Cellulose ethers. In: Mark HF, editor. Encyclopedia of polymer science and technology, vol. 5. New York: John Wiley and Sons; 2004. p. 503–31.
[43] Yamamoto H, Horii F, Hirai A. In situ crystallization of bacterial cellulose II. Influences of different polymeric additives on the formation of cellulose Iα and Iβ at the early stage of incubation. Cellulose 1996;3:229–42.
[44] Koutsopoulos S. Synthesis and characterization of hydroxyapatite crystals: a review study on the analytical methods. J Biomed Mater Res 2002;62:600–12.
[45] Sukhodub LF, Moseke C, Sukhodub LB, Sulkio-Cleff B, Maleev VY, Semenov MA, et al. Colllagen–hydroxyapatite–water interactions investigated by XRD, piezogravimetry, infrared and Raman spectroscopy. J Mol Struct 2004;704:53–8.
[46] Marechal Y, Chanzy H. The hydrogen bond network in Iβ cellulose as observed by infrared spectroscopy. J Mol Struct 2000; 523:183–96.
[47] Kacurakova M, Smith AC, Gidley MJ, Wilson RH. Molecular interactions in bacterial cellulose nanocomposites studied by 1D FT-IR and dynamic 2D FT-IR spectroscopy. Carbohydr Res 2002; 337:1145–53.
[48] Zhitomirsky I, Gal-Or L. Electrophoretic deposition of hydroxyapatite. J Mater Sci Mater Med 1997;8:213–9.
[49] Watanabe K, Tabuchi M, Morinaga Y, Yoshinaga F. Structural features and properties of bacterial cellulose produced in agitated culture. Cellulose 1998;5:187–200.
[50] Bhattarai SJ, Bhattarai N, Yi HK, Hwang PH, Cha DI, Kim YH. Novel biodegradable electrospun membrane: scaffold for tissue engineering. Biomaterials 2005;25:2595–602.
[51] Yang S, Leong KF, Du Z, Chua CK. The design of scaffolds for use in tissue engineering. Part I. Traditional factors. Tissue Eng 2001; 7:679–89.